

Article

One-Step Potentiostatic Deposition of Micro-Particles on Al Alloy as Superhydrophobic Surface for Enhanced Corrosion Resistance by Reducing Interfacial Interactions

Tian Shi ¹, Xuewu Li ^{1,*}, Qiaoxin Zhang ^{2,*} and Ben Li ²

¹ School of Mechanical Engineering, Xi'an University of Science and Technology, 58 Yanta Road, Xi'an 710054, China; tianshi@xust.edu.cn

² School of Mechanical and Electronic Engineering, Wuhan University of Technology, 122 Luoshi Road, Wuhan 430070, China; li_dd21@163.com

* Correspondence: lixuewu55@126.com (X.L.); zhangqx@whut.edu.cn (Q.Z.); Tel.: +86-29-85583159 (X.L.); +86-27-87859133 (Q.Z.); Fax: +86-29-83856323 (X.L.); +86-27-87651796 (Q.Z.)

Received: 30 August 2018; Accepted: 1 November 2018; Published: 5 November 2018



Abstract: Corrosion failure is a thorny problem that restricts the application of Al alloys. As a new technique for functional realization, hydrophobic preparation offers an efficient approach to solve corrosion problem. This work has developed a facile and low-cost method to endow Al alloy with enhanced water-repellent and anticorrosion abilities. The micro-particles have been firstly prepared by one-step deposition process. Furthermore, wetting and electrochemical behaviors of as-prepared structures have been investigated after silicone modification. Results show that the fabricated surface possesses excellent superhydrophobicity with a water contact angle (CA) of 154.7° and a sliding angle (SA) of 6.7°. Meanwhile, the resultant surface is proved with enhanced corrosion resistance by reducing interfacial interactions with seawater, owing to newly-generated solid-air-liquid interfaces. This work sheds positive insights into extending applications of Al alloys, especially in ocean engineering fields.

Keywords: Al alloy; superhydrophobicity; deposition; corrosion resistance; interfacial interaction

1. Introduction

Al alloys have aroused great interests due to their easy accessibility, low price, good process ability, and high specific strength [1–3]. Especially, they have been widely used as engineering components, parts and plates in shipbuilding, and ocean engineering areas [4,5]. Generally, Al alloys are easily oxidized to protect themselves from corrosion [6,7]. However, in wet conditions, reactive anions can erode metallic substrates leading to corrosion failures. Therefore, their application fields and service lives are seriously restricted. Based on these, it is of great economic value and practical significance to conduct the study of protecting Al alloys from corrosion in seawater.

In recent years, various methods of protective coating [8,9], corrosion inhibitor [10,11], aging process [12,13], mechanical alloying [14], laser treatment [15,16], micro-arc oxidation [17], phosphating process [18], and friction stir welding [19,20] have been reported to enhance the corrosion resistance of Al alloys. However, some coating protection processes with heavy metal ions are bad for environment. Phosphating technology is also contaminative. Laser treatment is usually costly and uncontrollable. Some other methods may be complicated. Therefore, developing a facile, low-cost, and environment-friendly anticorrosion method for Al alloys is still a big challenge.

Enlightened by the natural water-repelling and self-cleaning behaviors of lotus leaves [21,22], fabricating superhydrophobic layers on Al alloys can reduce interfacial interactions with corrosive

mediums, thereby slowing down their corrosion rates, which is a promising anticorrosion method. In general, a superhydrophobic surface can be achieved with a CA larger than 150° and a SA smaller than 10° [23–25]. Till now, various methods of sol-gel process [26], immersion process [27], in situ growth [28], hydrothermal treatment [29], chemical etching [30], spraying process [31], and laser marking technique [32] have been developed to prepare superhydrophobic Al alloys. Besides, Li et al. have fabricated a superhydrophobic Al foil with three-step immersion processes involving etching in hydrochloric acid, immersing in hot water, and surface modification in stearic acid [33]. Liu et al. have prepared a superhydrophobic 5052 Al alloy with a good repelling behavior to water after electrochemical anodic oxidation and chemical etching [34]. Li et al. have reported a superhydrophobic Al plate via etching, subsequent replacement deposition, and then annealing process [35]. However, corrosion resistances of samples in seawater are seldom mentioned in the above works. In addition, some methods are conducted under poor and complicated multi-step conditions to fabricate hydrophobic surfaces.

In this work, a simple and low-cost method is developed to prepare multifunctional Al alloys. The micro-particles on Al alloy surface have been prepared with the one-step potentiostatic deposition process. After silicone modification of rough structures, a self-assembled [36,37] low-surface-energy monolayer, as well as a superhydrophobic surface, has been attained. Finally, its corrosion resistance in seawater is confirmed by using electrochemical tests. The resultant surface exactly helps to reduce interfacial interactions with corrosive mediums, owing to the resultant composite solid-air-liquid interfaces. Such work sheds positive insights into extending applications of Al alloys, especially in shipbuilding and ocean engineering fields.

2. Materials and Methods

2.1. Materials

The commercially available 5005 Al alloys plates (10 mm × 10 mm × 2 mm) were used. The chemical compositions were listed in Table 1. 1H,1H,2H,2H-Perfluorodecyltrichlorosilane modifier (FAS) was purchased from Tokyo Chemical Industry Co., Ltd., Tokyo, Japan. Other reagents of analytical grade were obtained from Sinopharm Chemical Reagent Co., Ltd., Shanghai, China.

Table 1. The chemical compositions (in wt.%) of 5005 Al alloy.

Element	Mg	Fe	Mn	Zn	Cu	Si	Cr	Al
wt.%	1.5	0.7	0.2	0.2	0.2	0.1	0.1	97.0

2.2. Preparation

Firstly, Al alloys were polished with #320, #600, and #1600 sandpapers. After that, they were ultrasonically cleaned in ethanol and deionized water. Then, the potentiostatic deposition was carried out into 30 mM AgNO₃ solution at -0.50 V for 120 s. The deposition process was conducted by an electrochemical workstation (CHI660D, Chenhua Instrument Co., Ltd., Shanghai, China). A standard three-electrode system was used. Finally, the as-prepared samples were dried with high pure nitrogen and surface modification was conducted by immersing them into 10 mL ethanol solution of 20 mM FAS for 12 h. After that, they were dried in an oven at 100°C for 2 h before further tests. All of the processes were prepared at room temperature.

2.3. Characterization

Environmental Scanning Electron Microscopy (FESEM, FEI Quanta200 FEG, Hillsboro, OR, USA) was used to observe morphologies. Energy Dispersive X-ray Spectrometer (EDX, Oxford Instruments Inca X-Max, Oxfordshire, UK) was employed to analyze element compositions. Contact Angle Meter (OCA20, Dataphysics GmbH, Filderstadt, Germany) was used to measure CA and SA

values. Their average values were tested at five various spots for each sample. Electrochemical workstation (CHI660D, Chenhua Instrument Co., Ltd., Shanghai, China) was employed to evaluate corrosion resistance in 3.5 wt.% NaCl solution. Electrochemical impedance spectroscopy (EIS) was tested between 10 mHz and 100 kHz, with a sine wave amplitude of 10 mV. The polarization curve was recorded from -1600 to -400 mV with a scanning rate of 1 mV/s. To achieve steady states, working electrodes were immersed into electrolyte for 30 min before electrochemical tests.

3. Results and Discussion

3.1. Fabrication of Superhydrophobic Surfaces

Figure 1 shows SEM images of Al alloy substrate and the deposited sample. As seen, a relatively smooth surface is observed on metallic substrate (Figure 1a). After the deposition process, uniformly dispersed micro-particles form on Al alloy surface with average film thickness of 100–150 μm and characteristic dimension of 1–2 μm , as seen in Figure 1b. The growth process of particles greatly lies on deposition process. To begin with, nucleation sites with silver buds take shapes due to a reduction reaction in AgNO_3 solution. Then, nucleation tips with low energy promote more buds attachment resulting in aggregated nuclei and eventually forming micro-particles. XRD analysis is also conducted to determine the crystal structures of deposited particles, as seen in Figure 1c. By comparing with standard JCPDS card (4-783), the characteristic peaks are indexed as (111), (200), (220), (311), and (222) crystal planes indicating the face-centered cubic structures of silver particles.

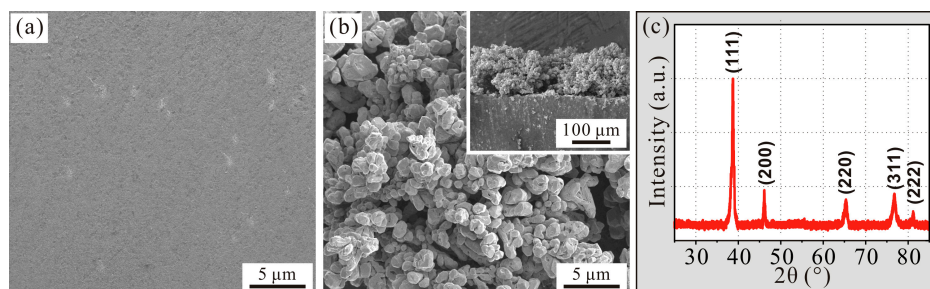


Figure 1. SEM images of (a) Al alloy substrate and (b) deposited sample. (c) XRD spectrum of deposited surface. The insert in (b) referring to cross-sectional image of deposited sample.

Generally, FAS modification is an effective method to fabricate low-surface-energy coating [38]. Figure 2 displays wet abilities of various Al alloy samples. Clearly, a hydrophilic substrate is observed in Figure 2a,b. Contrastively, the modified deposited surface is prepared with a superhydrophobic CA of 154.7° (Figure 2c), which looks like a spherical water drop standing on sample (Figure 2d). In fact, Wenzel model demonstrates that rough structures have a positive effect on water repellence [39]. Just owing to the enhanced roughness of micro-particles (Figure 3), the deposited sample is advantageous to achieve superhydrophobicity over smooth Al alloy substrate.

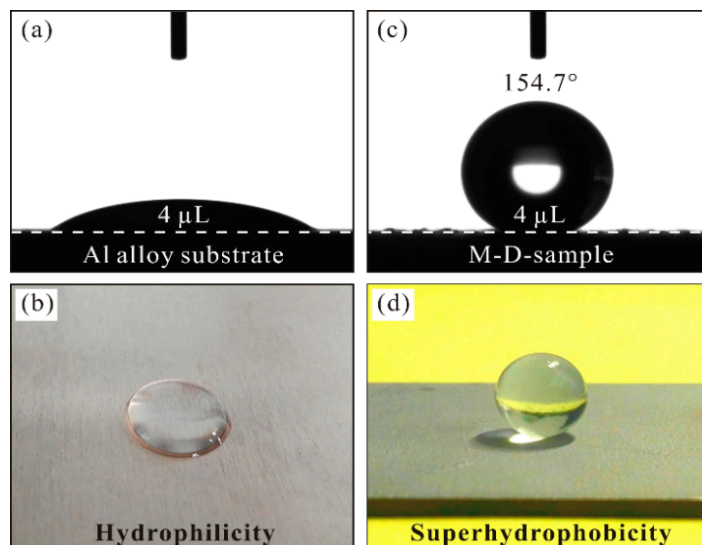


Figure 2. Water contact angles of (a) substrate and (c) modified deposited sample (M-D-sample). Optical photos of droplets (20 μL) on (b) substrate and (d) modified deposited sample.

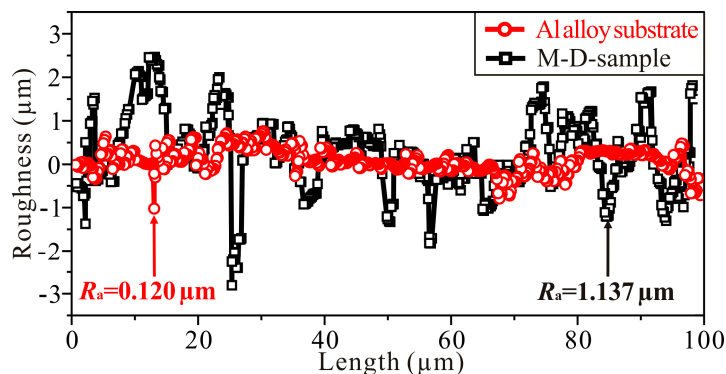


Figure 3. Roughnesses of Al alloy substrate and modified deposited sample (M-D-sample).

In addition, SA is also an essential parameter for evaluating superhydrophobicity [40]. As seen in Figure 4a, the droplet still adheres to metallic substrate even when it turns over, indicating a strong water adhesion. But, for modified deposited surface, a small SA of 6.7° is obtained (Figure 4b), which indeed shows excellent water repellence. To further investigate the significance of as-prepared micro-particles on superhydrophobicity, the wettability of modified Al alloy substrate without pre-deposited Ag film is presented in Figure 4c. As seen, after FAS modification of hydrophilic Al alloy substrate, a hydrophobic CA of 98.3° is achieved. Hence, the potentiostatic deposition of Ag particles is necessary to the following FAS modification to achieve superhydrophobicity.

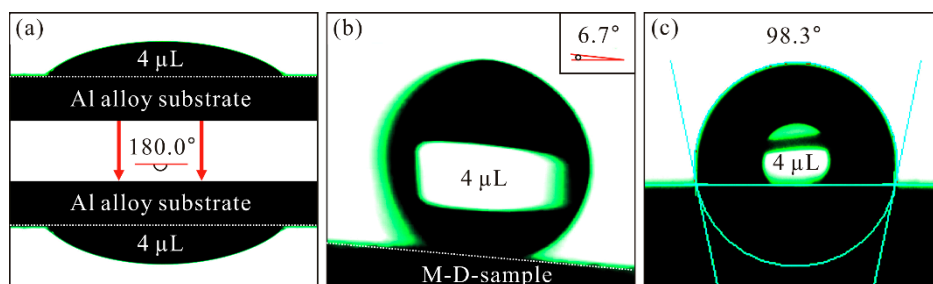


Figure 4. Sliding angles of (a) Al alloy substrate and (b) modified deposited sample (M-D-sample). (c) Water contact angles of modified substrate.

As an attempt to gain insights into as-prepared surfaces, EDX spectra and SEM images of the deposited Al alloys before and after FAS modification are shown in Figure 5. As seen, inconspicuous differences in morphologies are identified before and after modification, indicating few effects of FAS layer on micro-particles. Besides, the deposited surface is mainly composed of the Al, Mg, O, as well as Ag element (Figure 5a), which comes from micro-particles fabricated in deposition process. After the modification process, new elements of F and Si are seen (Figure 5b) suggesting that FAS membrane is successfully incorporated on deposited surface. The formation of FAS layer can be exactly described as the derived process of a self-assembled monolayer [36,37]. In general, fluorine is highly electrophilic, thereby giving C–F bond strong chemical inertia and FAS layer low surface energy [41]. Consequently, the resultant surface is prepared with superhydrophobicity, which is also conducive to repel liquids.

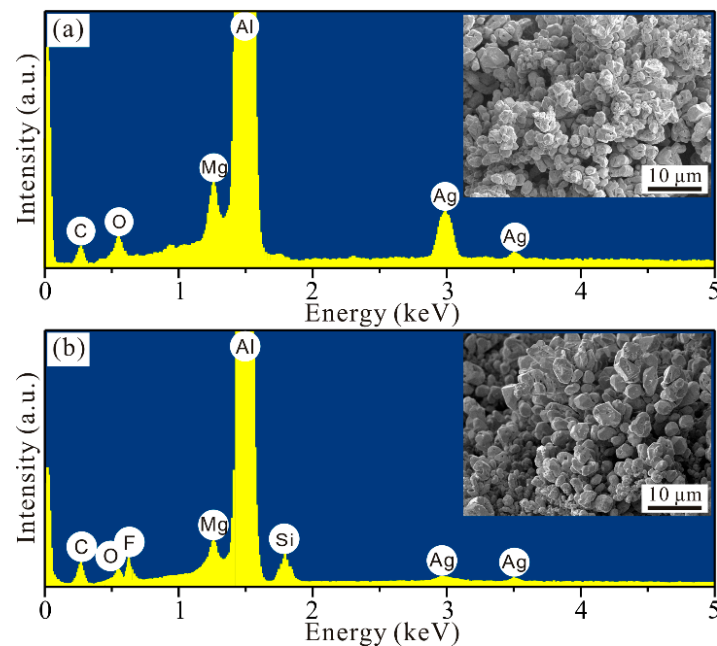


Figure 5. Energy Dispersive X-ray Spectrometer (EDX) spectra and SEM images of deposited Al alloys (a) before and (b) after 1H,1H,2H,2H-Perfluorodecyltrichlorosilane modifier (FAS) modification.

3.2. Anticorrosion Behaviors of as-Prepared Al Alloys

Figure 6 shows the anticorrosion abilities of Al alloy substrate, deposited samples before and after FAS modification characterized by potentiodynamic polarization curves. In general, a surface with a positive-shifting corrosion potential (E) and a low corrosion current density (I) is provided with superior corrosion resistance [42]. Obviously, current densities for the deposited sample, substrate, and modified deposited sample are 4.73, 3.06, and 0.98 $\mu\text{A}/\text{cm}^2$, respectively. Meanwhile, corrosion potentials shift positively from -1.24 , -1.21 , to -0.86 V for above samples. These data shows evidence that the corrosion resistance of such deposited sample has been greatly enhanced after modification and the resultant surface also achieves the best anticorrosion ability.

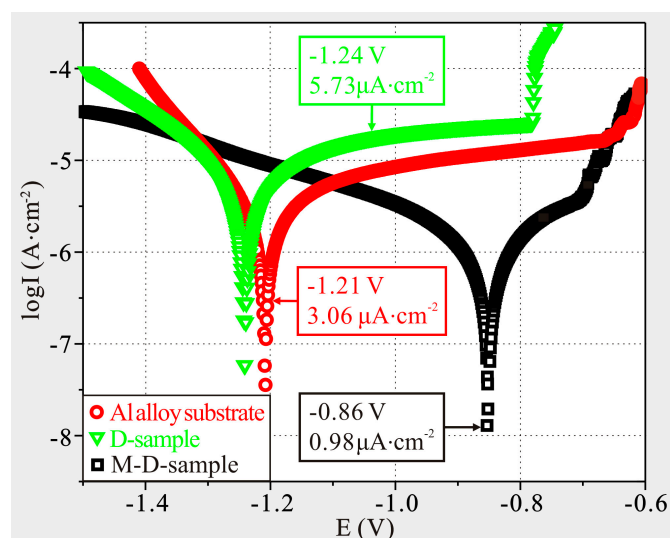


Figure 6. Potentiodynamic polarization curves of Al alloy substrate, deposited sample (D-sample) and modified deposited sample (M-D-sample).

Al alloy substrate displays poor corrosion resistance. This is due to the reactive anions abundant in seawater, which directly erodes metallic substrate thereby leading to corrosion failures (Figure 7a). But, for modified deposited sample, an enhanced corrosion resistance is achieved. As is known, fluorine has strong polarity endowing C–F bond with strong chemical inertness [41]. As a result, FAS film displays low surface energy to repel liquids. Meanwhile, CH groups of absorbed FAS molecules have a good ability of anti-OH bonds, thereby intensifying such liquid repellence [43]. Due to above functional groups, the assembled FAS layer guarantees as-prepared surface superior superhydrophobicity and also obstructs seawater penetrations by impeding interfacial interactions with corrosive ions. On the other hand, the as-prepared superhydrophobic micro-particles are propitious to improve the chance for trapping air (Figure 7b). The air phase can exactly serve as dielectric for a parallel plate capacitor, which can keep the electrons from transferring between seawater and sample. Based on such reasons, the resultant sample has been prepared with enhanced corrosion resistance.

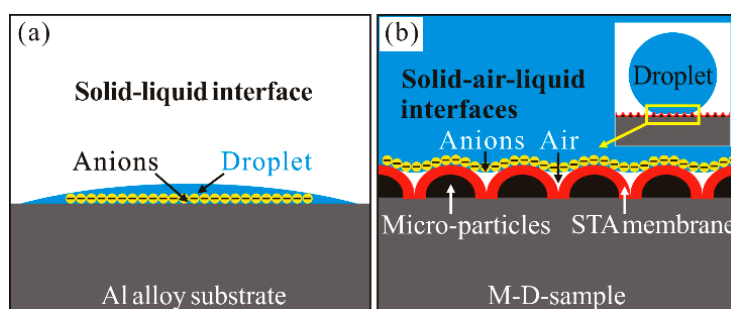


Figure 7. Interfacial relationships of (a) Al alloy substrate and (b) modified deposited sample.

EIS analyses can also be used to evaluate corrosion resistances. Figure 8 shows the resultant Nyquist plots of Al alloy substrate, deposited sample, and modified deposited sample. In Nyquist plots, semicircles relate to capacitance arcs, which can be used to assess polarization resistances. Meanwhile, a big capacitance arc signifies a large polarization resistance as well as a better impeditive ability to transfer electrons [42], which also suggests a superior corrosion resistance. It is clearly seen that the capacitance arc for modified deposited sample is larger than others, and the same goes for anticorrosion ability. Hence, the same trend about electrochemical result that is displayed in polarization curve is also found in such EIS measurement.

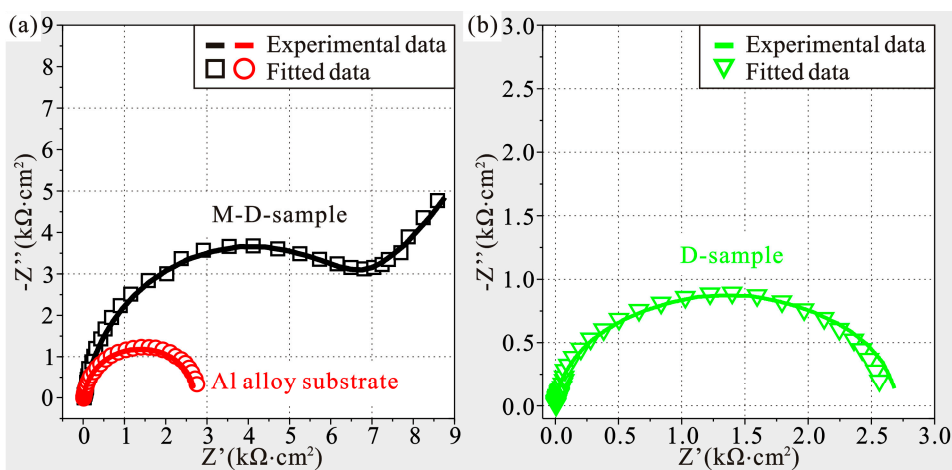


Figure 8. Experimental and fitted Nyquist plots of (a) Al alloy substrate, modified deposited sample (M-D-sample) and (b) deposited sample (D-sample).

To determine electrochemical data of Al alloy substrate, deposited sample, and modified deposited sample, ZSimDemo software is used to fit EIS curves. After fittings, the circuit model $R_s(R_{ct1}C_{dl})$ in Figure 9a is found appropriate to equate electrochemical process of metallic substrate and deposited sample in seawater. In such pattern, C_{dl} , R_{ct1} , and R_s , respectively, refer to double-layer capacitance, charge-transfer resistance, and solution resistance. The model $R_s(C_c(R_c(C_{dl}(R_{ct2}W))))$ in Figure 9b is found to be suitable to fit EIS curves of modified deposited sample, where R_c and C_c respectively denote resistance and capacitance of the modified film. In an electrode process, solution concentration is different from reactant concentration on electrode surface thereby leading to reactant diffusion from solution to electrode surface. In this pattern, the diffusion impedance (W) is used to characterize the inhibitory ability of such a diffusion process. As seen, the fitted curves (Figure 8) can well match experimental results indicating reasonable fittings of EIS plots in this work. In fitting process, the electrochemical data are also achieved and listed in Table 2. After comparison and analysis, the modified deposited sample is provided with the largest polarization resistance ($R_t = R_{ct} + R_c$) and diffusion impedance suggesting the strongest inhibitory actions of reactant diffusions and charge transfers, as well as the best corrosion resistance, which coincides well with the experimental results. In brief, the corrosion resistance of Al alloy is greatly enhanced by reducing interfacial interactions with seawater after deposition and modification processes in this work.

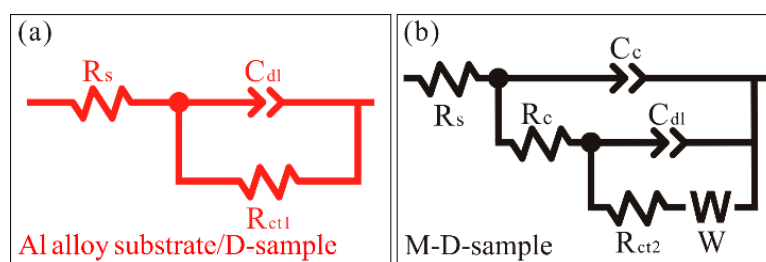


Figure 9. Equivalent circuit patterns of (a) Al alloy substrate, deposited sample (D-sample) and (b) modified deposited sample (M-D-sample).

Table 2. Fitted electrochemical parameters of Al alloy substrate, deposited sample (D-sample), and modified deposited sample (M-D-sample).

Samples	R_s ($\Omega \cdot cm^2$)	R_{ct} ($\Omega \cdot cm^2$)	R_c ($\Omega \cdot cm^2$)	R_t ($\Omega \cdot cm^2$)	W ($\Omega \cdot cm^2$)
Substrate	12	2690	–	2690	–
D-sample	9	2416	–	2416	–
M-D-sample	10	7105	437	7542	0.0028

The stabilities of superhydrophobicity and corrosion resistance in seawater are investigated for the modified deposited sample in Figure 10. Clearly, after 30 days immersion, CA, SA, E , I , and surface topographies all maintain relatively stable levels suggesting excellent durability in seawater. Hence, the durable corrosion resistance of Al alloy resulting from its superhydrophobic stability is achieved to expand its potential applications as engineering materials in corrosive environments.

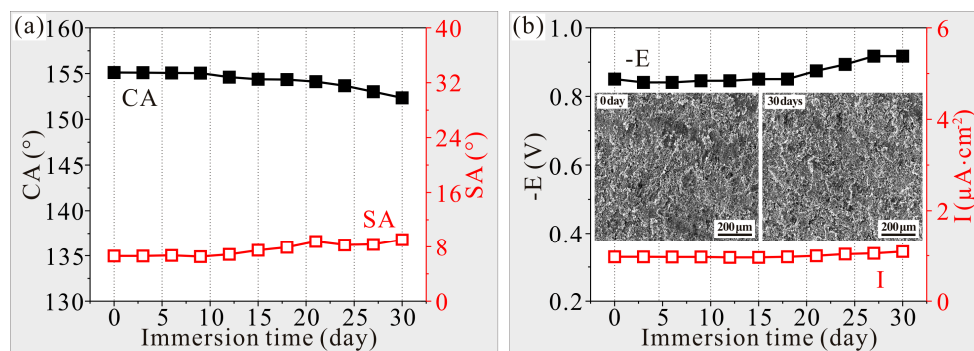


Figure 10. Effects of immersion time in seawater on (a) wettability and (b) corrosion resistance of modified deposited sample. The inserts in (b) referring to SEM images of modified deposited sample after immersion in seawater for 0 day and 30 days.

4. Conclusions

(1) Uniformly dispersed micro-particles with an average film thickness of 100–150 μm and characteristic dimension of 1–2 μm have been prepared on 5005 Al alloy surface by a facile potentiostatic deposition process in 30 mM silver nitrate solution at -0.50 V for 120 s.

(2) After fluoroalkylsilane modification, the as-prepared rough structures have displayed excellent water repellence with a water contact angle of 154.7° and a sliding angle of 6.7° .

(3) The superhydrophobic Al alloy surface has been prepared with greatly enhanced corrosion resistance in seawater by reducing the interfacial interactions between aggressive medium and modified deposited surface, owing to the resultant composite solid-air-liquid interfaces.

Author Contributions: Conceptualization, X.L. and Q.Z.; Methodology, T.S. and B.L.; Investigation, T.S. and B.L.; Writing-Original Draft Preparation, T.S. and B.L.; Writing-Review & Editing, X.L. and Q.Z.; Funding Acquisition, X.L.

Funding: The work is financially supported by the National Natural Science Foundation of China (Nos. 51875425, 51705416).

Acknowledgments: We would like to thank Chen Zhou and Dong Yu (Analytical & Testing Center, WHUT) for help in SEM observation and EDX analysis.

Conflicts of Interest: The authors declare no competing financial interest.

References

- Zhang, T.; Luo, H.Y.; Su, Y.Q.; Xu, P.W.; Luo, J.; Li, S.J. Effect of precipitate embryo induced by strain on natural aging and corrosion behavior of 2024 Al alloy. *Coatings* **2018**, *8*, 92. [[CrossRef](#)]
- Massardier, V.; Epicier, T.; Merle, P. Correlation between the microstructural evolution of a 6061 aluminium alloy and the evolution of its thermoelectric power. *Acta Mater.* **2017**, *48*, 2911–2924. [[CrossRef](#)]
- Choi, I.K.; Cho, S.H.; Kim, S.J.; Jo, Y.S.; Kim, S.H. Improved corrosion resistance of 5xxx aluminum alloy by homogenization heat treatment. *Coatings* **2018**, *8*, 39. [[CrossRef](#)]
- Katkar, V.A.; Gunasekaran, G. Galvanic corrosion of AA6061 with other ship building materials in seawater. *Corrosion* **2015**, *72*, 400–412. [[CrossRef](#)]
- Chen, M.D.; Zhang, F.; Liu, Z.Y.; Yang, C.H.; Ding, G.Q.; Li, X.G. Galvanic series of metals and effect of alloy compositions on corrosion resistance in Sanya seawater. *Acta Metall. Sin.* **2018**, *54*, 1311–1321.

6. Jedrusik, M.; Debowska, A.; Kopia, A. Characterisation of oxide coatings produced on aluminum alloys by MAO and chemical methods. *Arch. Metall. Mater.* **2018**, *63*, 125–128.
7. Kwolek, P.; Krupa, K.; Obloj, A.; Kocurek, P.; Wierzbinska, M.; Sieniawski, J. Tribological properties of the oxide coatings produced onto 6061-T6 aluminum alloy in the hard anodizing process. *J. Mater. Eng. Perform.* **2018**, *27*, 3268–3275. [[CrossRef](#)]
8. Liu, Y.Y.; Huang, J.M.; Claypool, J.B.; Castano, C.E.; O'Keefe, M.J. Structure and corrosion behavior of sputter deposited cerium oxide based coatings with various thickness on Al 2024-T3 alloy substrates. *Appl. Surf. Sci.* **2015**, *355*, 805–813. [[CrossRef](#)]
9. Serizawa, A.; Oda, T.; Watanabe, K.; Mori, K.; Yokomizo, T.; Ishizaki, T. Formation of anticorrosive film for suppressing pitting corrosion on Al-Mg-Si alloy by steam coating. *Coatings* **2018**, *8*, 23. [[CrossRef](#)]
10. Lin, J.; Battocchi, D.; Bierwagen, G.P. Inhibitors for prolonging corrosion protection of Mg-rich primer on Al alloy 2024-T3. *J. Coat. Technol. Res.* **2017**, *14*, 497–504. [[CrossRef](#)]
11. Hikku, G.S.; Jeyasubramanian, K.; Venugopal, A.; Ghosh, R. Corrosion resistance behaviour of graphene/polyvinyl alcohol nanocomposite coating for aluminium-2219 alloy. *J. Alloy. Compd.* **2017**, *716*, 259–269. [[CrossRef](#)]
12. Zhu, Y.; Ji, Q.Q.; Jin, M. Effects of non-isothermal aging process on mechanical properties and corrosion resistance of Al-Mg-Si aluminum alloy. *Mater. Corros.* **2018**, *69*, 634–640. [[CrossRef](#)]
13. Lin, Y.C.; Jiang, Y.Q.; Xia, Y.C.; Zhang, X.C.; Zhou, H.M.; Deng, J. Effects of creep-aging processing on the corrosion resistance and mechanical properties of an Al-Cu-Mg alloy. *Mater. Sci. Eng. A* **2014**, *605*, 192–202. [[CrossRef](#)]
14. Seikh, A.H.; Baig, M.; Ammar, H.R.; Alam, M.A. The influence of transition metals addition on the corrosion resistance of nanocrystalline Al alloys produced by mechanical alloying. *Metals* **2016**, *6*, 140. [[CrossRef](#)]
15. Ravnikar, D.; Rajamure, R.S.; Trdan, U.; Dahotre, N.B.; Grum, J. Electrochemical and DFT studies of laser-alloyed TiB₂/TiC/Al coatings on aluminium alloy. *Corros. Sci.* **2018**, *136*, 18–27. [[CrossRef](#)]
16. Yang, Y.; Chen, Y.; Zhang, J.X.; Gu, X.H.; Qin, P.; Dai, N.W.; Li, X.P.; Kruth, J.P.; Zhang, L.C. Improved corrosion behavior of ultrafine-grained eutectic Al-12Si alloy produced by selective laser melting. *Mater. Des.* **2018**, *146*, 239–248. [[CrossRef](#)]
17. Kaseem, M.; Yong, H.L.; Ko, Y.G. Incorporation of MoO₂, and ZrO₂, particles into the oxide film formed on 7075 Al alloy via micro-arc oxidation. *Mater. Lett.* **2016**, *182*, 260–263. [[CrossRef](#)]
18. Ji, S.P.; Weng, Y.C.; Wu, Z.Z.; Ma, Z.Y.; Tian, X.B.; Fu, R.K.Y.; Lin, H.; Wu, G.S.; Chu, P.K.; Pan, F. Excellent corrosion resistance of P and Fe modified micro-arc oxidation coating on Al alloy. *J. Alloy. Compd.* **2017**, *710*, 452–459. [[CrossRef](#)]
19. Navaser, M.; Atapour, M. Effect of friction stir processing on pitting corrosion and intergranular attack of 7075 aluminum alloy. *J. Mater. Sci. Technol.* **2017**, *2*, 155–165. [[CrossRef](#)]
20. Li, N.; Li, W.Y.; Xu, Y.X.; Yang, X.W.; Alexopoulos, N.D. Influence of rotation speed on mechanical properties and corrosion sensitivity of friction stir welded AA2024-T3 joints. *Mater. Corros.* **2018**, *69*, 1016–1024. [[CrossRef](#)]
21. Sebastian, D.; Yao, C.W.; Lian, I. Mechanical durability of engineered superhydrophobic surfaces for anti-corrosion. *Coatings* **2018**, *8*, 162. [[CrossRef](#)]
22. Li, X.W.; Zhang, Q.X.; Guo, Z.; Shi, T.; Yu, J.G.; Tang, M.K.; Huang, X.J. Fabrication of superhydrophobic surface with improved corrosion inhibition on 6061 aluminum alloy substrate. *Appl. Surf. Sci.* **2015**, *342*, 76–83. [[CrossRef](#)]
23. Bayer, I.S. On the durability and wear resistance of transparent superhydrophobic coatings. *Coatings* **2017**, *7*, 12. [[CrossRef](#)]
24. Wang, G.Y.; Liu, S.; Wei, S.F.; Liu, Y.; Lian, J.S.; Jiang, Q. Robust superhydrophobic surface on Al substrate with durability, corrosion resistance and ice-phobicity. *Sci. Rep.* **2016**, *6*, 20933. [[CrossRef](#)] [[PubMed](#)]
25. Li, X.W.; Liu, C.; Shi, T.; Lei, Y.J.; Zhang, Q.X.; Zhou, C.; Huang, X.J. Preparation of multifunctional Al alloys substrates based on micro/nanostructures and surface modification. *Mater. Des.* **2017**, *122*, 21–30. [[CrossRef](#)]
26. Lee, J.W.; Hwang, W. Exploiting the silicon content of aluminum alloys to create a superhydrophobic surface using the sol-gel process. *Mater. Lett.* **2016**, *168*, 83–85. [[CrossRef](#)]
27. Ishizaki, T.; Kumagai, S.; Tsunakawa, M.; Furukawa, T.; Nakamura, K. Ultrafast fabrication of superhydrophobic surfaces on engineering light metals by single-step immersion process. *Mater. Lett.* **2017**, *193*, 42–45. [[CrossRef](#)]

28. Zhang, Y.; Liu, J.H.; Li, Y.D.; Yu, M.; Li, S.M.; Xue, B. A facile approach to superhydrophobic LiAl-layered double hydroxide film on Al-Li alloy substrate. *J. Coat. Technol. Res.* **2015**, *12*, 595–601. [[CrossRef](#)]
29. Li, L.J.; Huang, T.; Lei, J.L.; He, J.X.; Qu, L.F.; Huang, P.L.; Zhou, W.; Li, N.B.; Pan, F.S. Robust biomimetic-structural superhydrophobic surface on aluminum alloy. *ACS Appl. Mater. Interfaces* **2014**, *7*, 1449–1457. [[CrossRef](#)] [[PubMed](#)]
30. Zhang, Q.H.; Jim, B.Y.; Wang, B.; Fu, Y.C.; Zhan, X.L.; Chen, F.Q. Fabrication of a highly stable superhydrophobic surface with dual-scale structure and its antifrosting properties. *Ind. Eng. Chem. Res.* **2017**, *56*, 2754–2763. [[CrossRef](#)]
31. Belsanti, L.; Ogihara, H.; Mahanty, S.; Luciano, G. Electrochemical behaviour of superhydrophobic coating fabricated by spraying a carbon nanotube suspension. *Bull. Mater. Sci.* **2015**, *38*, 579–582. [[CrossRef](#)]
32. Tang, M.K.; Huang, X.J.; Guo, Z.; Yu, J.G.; Li, X.W.; Zhang, Q.X. Fabrication of robust and stable superhydrophobic surface by a convenient, low-cost and efficient laser marking approach. *Colloids Surf. A* **2015**, *484*, 449–456. [[CrossRef](#)]
33. Li, P.P.; Chen, X.H.; Yang, G.B.; Yu, L.G.; Zhang, P.Y. Fabrication and characterization of stable superhydrophobic surface with good friction-reducing performance on Al foil. *Appl. Surf. Sci.* **2014**, *300*, 184–190. [[CrossRef](#)]
34. Le, Y.; Dale, B.; Akisik, F.; Koons, K.; Lin, C. Preparation and anti-icing behavior of superhydrophobic surfaces on aluminum alloy substrates. *Langmuir* **2013**, *29*, 8482–8491.
35. Li, J.Y.; Lu, S.X.; Xu, W.G.; He, G.; Yu, T.L.; Cheng, Y.Y.; Wu, B. Fabrication of stable Ni-Al₄Ni₃-Al₂O₃ superhydrophobic surface on aluminum substrate for self-cleaning, anti-corrosive and catalytic performance. *J. Mater. Sci.* **2018**, *53*, 1097–1109. [[CrossRef](#)]
36. Ou, J.; Hu, W.; Xue, M.; Wang, F.; Li, W. One-step solution immersion process to fabricate superhydrophobic surfaces on light alloys. *ACS Appl. Mater. Interfaces* **2013**, *5*, 9867–9871. [[CrossRef](#)] [[PubMed](#)]
37. Saleema, N.; Sarkar, D.K.; Gallant, D.; Paynter, R.W.; Chen, X.G. Chemical nature of superhydrophobic aluminum alloy surfaces produced via a one-step process using fluoroalkyl-silane in a base medium. *ACS Appl. Mater. Interfaces* **2011**, *3*, 4775–4781. [[CrossRef](#)] [[PubMed](#)]
38. Cai, Y.W.; Li, S.; Cheng, Z.L.; Xu, G.Y.; Quan, X.J.; Zhou, Y.T. Facile fabrication of super-hydrophobic FAS modified electroless Ni-P coating meshes for rapid water-oil separation. *Colloids Surf. A* **2018**, *540*, 224–232. [[CrossRef](#)]
39. Lee, C.; Nam, Y.; Lastakowski, H.; Hur, J.I.; Shin, S.; Biance, A.L.; Pirat, C.; Kim, C.J.; Ybert, C. Two types of cassie-to-wenzel wetting transitions on superhydrophobic surfaces during drop impact. *Soft Matter* **2015**, *11*, 4592–4599. [[CrossRef](#)] [[PubMed](#)]
40. Wang, J.; Chen, H. Preparation and anti-icing property of a porous superhydrophobic magnesium oxide coating with low sliding angle. *Adv. Mater. Res.* **2012**, *557–559*, 1884–1887. [[CrossRef](#)]
41. Shi, T.; Kong, J.Y.; Wang, X.D.; Li, X.W. Preparation of multifunctional Al-Mg alloy surface with hierarchical micro/nanostructures by selective chemical etching processes. *Appl. Surf. Sci.* **2016**, *389*, 335–343. [[CrossRef](#)]
42. Li, X.W.; Shi, T.; Liu, C.; Zhang, Q.X.; Huang, X.J. Multifunctional substrate of Al alloy based on general hierarchical micro/nanostructures: Superamphiphobicity and enhanced corrosion resistance. *Sci. Rep.* **2016**, *6*, 35940. [[CrossRef](#)] [[PubMed](#)]
43. Min, R.; Li, W.; Wang, B.; Luo, Q.; Ma, F.M.; Yu, Z.L. Optimal conditions for the preparation of superhydrophobic surfaces on Al substrates using a simple etching approach. *Appl. Surf. Sci.* **2012**, *258*, 7031–7035.

